Chapter 18
Experimental Characterization of Semi-Rigidity of Standardized Lattice Beam Using the Grid Method

Eric Fournely, Rostand Moutou Pitti, Evelyne Toussaint, and Michel Grediac

Abstract Timber structures often exhibit shear and tension perpendicular to grain. This phenomenon induces brittle failure if it is not controlled. This is particularly the case in joining zones, and even more when the beam elements are thin. These thin elements can be found for example in lattice beams. Standardized lattice timber beams appear as an efficient solution for economical, ecological and mechanical aspects. This study focuses on the mechanical behavior of notched beams. Experiments are carried out with a classic loading device and LVDT measurements as well as with the grid method which provides full-field displacement and strain measurements. Tests are conducted for various orientations of annual rings of the wood. The evolutions of strains in the zone affected by shear and tension stresses are analyzed.

Keywords Notched beam • Grid method • Experimental analysis

18.1 Introduction

In wood material, shear and tension perpendicular to grain generally induce brittle fracture if they are not controlled. This is particularly the case in joining zones and even more when the beam elements are thin. These thin elements can be found for example in lattice beams [1, 2]. Standardized lattice timber beams appear as an efficient solution for economical, ecological and mechanical reasons. Many uses of this type of structure can be found in the field of industrial buildings as well as in small and collective housings. This study focuses on the stress distribution in notched beams specimens cut in chord elements of a timber truss beam previously studied with various connector or adhesives [3]. The orientation of the annual rings, the direction of the grain and the knot area ratio are important parameters which drive the global mechanical behavior of theses beams.

In the literature, few authors have shown the influence of the connections [1, 4] on the global behavior of structures and especially of timber structures. In fact, digital image correlation is generally employed in order to evaluate mechanical displacements during the test [5]. The present work is aimed at studying the mechanical behavior of notched beams using another measurement technique, namely the grid method [6]. This method has been recently successfully employed in various cases such as the characterization of notched aluminum specimens [7] or the failure of wooden specimens for instance [8, 9]. In particular, the grid method enables one to obtain here the evolution of the strain field in the zone affected by shear and tension stresses.

E. Fournely • E. Toussaint
LaMI - CNRS - Blaise Pascal University, BP 265 - Campus de Cezeaux, Aubiere Cedex 63175, France

M. Grediac
LaMI, Campus de Clermont-Ferrand, Les Cezeaux, BP 265, Aubiere Cedex 63175, France

R. Moutou Pitti (✉)
Universite Blaise Pascal, Polytech Clermont-Ferrand, 24 Avenue des Landais, PB 206, Aubiére, Auvergne 63174, France
e-mail: rostand.moutou_pitti@puniv-bpclermont.fr

J. Carroll and S. Daly (eds.), *Fracture, Fatigue, Failure, and Damage Evolution, Volume 5: Proceedings of the 2014 Annual Conference on Experimental and Applied Mechanics*, Conference Proceedings of the Society for Experimental Mechanics Series,
DOI 10.1007/978-3-319-06977-7_18, © The Society for Experimental Mechanics, Inc. 2015

The wood specimens and the different orientations of the annual rings are presented in the first part of the paper. Various configurations tests, the experimental procedure, the experimental device and the grid technique are then recalled. Then, the deformations and the displacements maps located at the support point, where cracks can be appear and growth, are shown and discussed.

18.2 Experimental Setup

18.2.1 Specimen and Loading Conditions

Numerous tests on notched beams were carried out on Zwick testing machine. A schematics of the test is shown in Fig. 18.1. The forces were measured by two 5 kN sensors. One of these sensors is placed at the center, at point B where force F1 is applied; the second is placed at point A where F2 is applied. Force F3 located at point C is calculated as the difference of the previous two forces. For the boundary conditions, two spherical contacts placed at points A and B enable us to avoid any potential parallelism defects between the notched face and the faces where F1 and F2 are applied. The support plate is fixed close to the notch; its width is 20 mm. The quick trimmer (UPE80) provides the support of the force sensor and position of the central displacement sensor, which records the global deflection. A second sensor records the evolution of beam's height near the notch. The dimensions shown in Fig. 18.1 are in agreement with the configuration described before. Figure 18.2 shows a picture of the specimen in real configuration test with the testing machine.

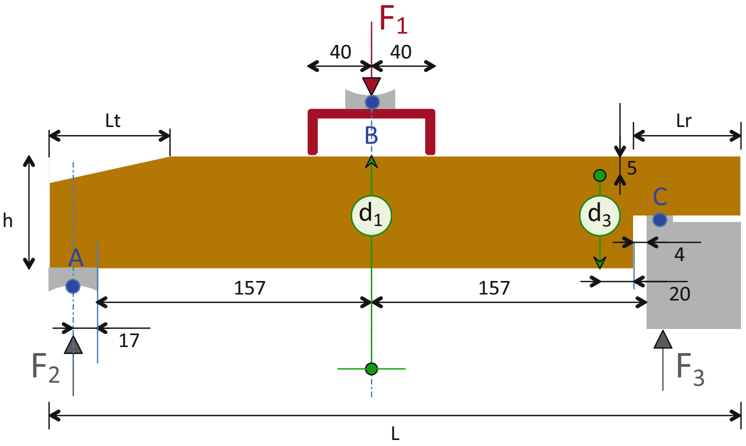

Fig. 18.1 Configuration and geometry of experimental tests

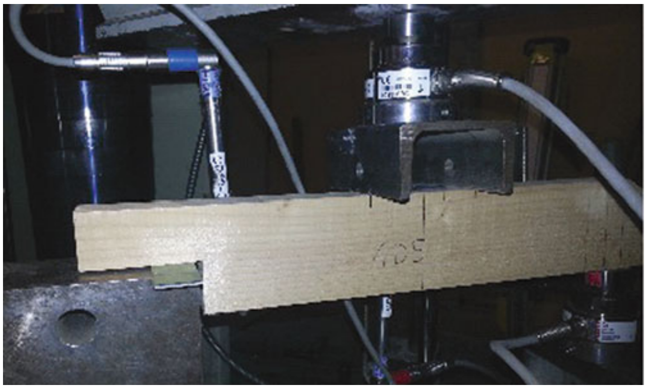

Fig. 18.2 Real experimental device

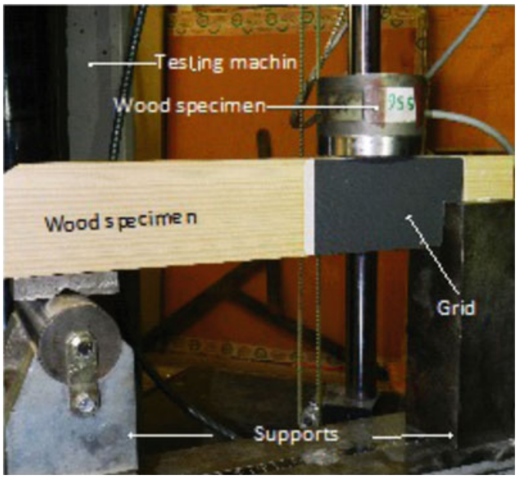

Fig. 18.3 Experimental device with grid

18.2.2 *The Grid Method*

The grid method consists first in depositing a crossed grid on the surface under investigation in order to track the slight change in the grid as loading increases. The 2D displacement and strain fields are deduced from the images of the grid taken during the test. The grid is deposited using the procedure described in [10]. The pitch of the grid is equal here to 0.2 mm along both directions. Processing images of the grid classically provides phase and phase derivative change maps of this quasi-periodical marking. These quantities are directly proportional to the in-plane displacement and strain components, respectively. It has been shown that the metrological performance of this technique could be significantly improved (especially for strain measurements) by getting rid of most of the grid marking defects, which unavoidably occur when grids are printed on their polymeric support before transfer on the specimen [6]. This leads to a good compromise between resolution and spatial resolution of the measurements. In the current case, a 12-bit/1,040 × 1,376 pixel SENSICAM camera connected to its companion software CamWare is employed. The strain maps are obtained directly from the images of the grids taken by the camera. Full details on small strain calculation can be found in Ref. [6].

Figure 18.3 presents the experimental device employed during the tests. The wood specimen in bending can be seen as well as the load sensor and the supports of a classic 200 kN testing machine.

18.3 Results and Discussions

Typical horizontal and vertical displacement fields measured before crack appearance are shown in Figs. 18.4 and 18.5, respectively. Dimensions are given in pixels (1 pixel = 40 μm). These fields are rather smooth despite the small spatial resolution employed in the grid image processing. This spatial resolution can be estimated to be equal to 30 pixels only. The magnitude of the displacement is small too: some tenths of mm only but the maps are not noisy. The impact of the annual rings is not visible on these displacement maps.

The ε_{xy} and ε_{yy} strain maps are shown in Figs. 18.6 and 18.7 (the ε_{xx} maps is not considered here because of the too low amplitude of this quantity). These maps are obtained at the same loading level as the displacement maps discussed above. The effect of the material heterogeneity due to the annual rings is clearly visible, especially in the ε_{yy} map : the transverse tensile strain strongly changes from one ring to each other. This transverse tensile straining causes a crack to appear at the corner of the notch for a higher loading level, and then to propagate horizontally.

18.4 Conclusion

This paper presents an experimental study on notched thin beam with thin different configurations. Strength values obtained in this experimentation study are in a good agreement with EN1995.1.1 predictions. Grid method analysis exhibits interesting results in order to give more information on lattice beams with equivalent cross-section chord beams. This extension will be completed soon by a FEM analysis.

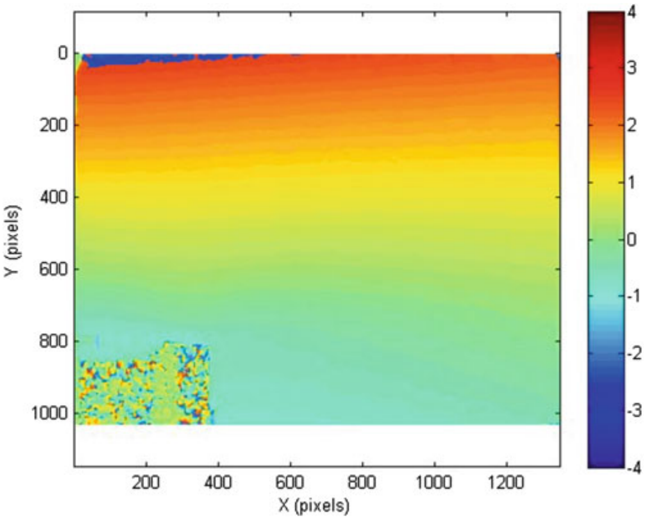

Fig. 18.4 Typical horizontal displacement field (all dimensions in pixel, 1 pixel = 40 μm)

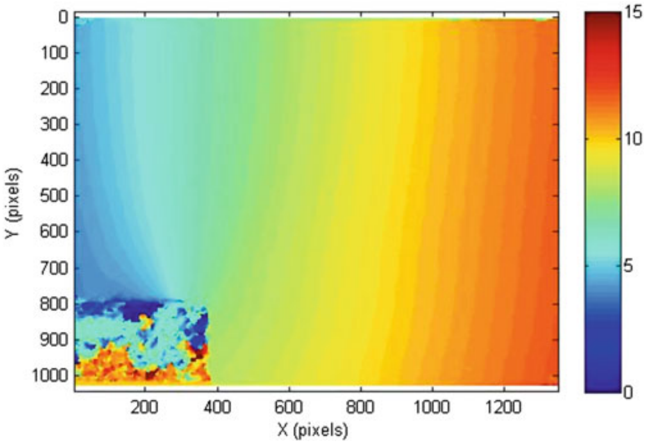

Fig. 18.5 Typical vertical displacement field (all dimensions in pixel, 1 pixel = 40 μm)

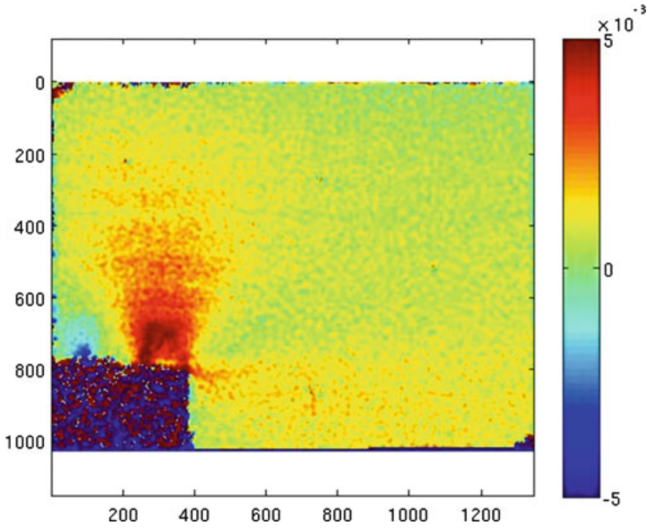

Fig. 18.6 ε_{xy} map

Fig. 18.7 ε_{yy} map

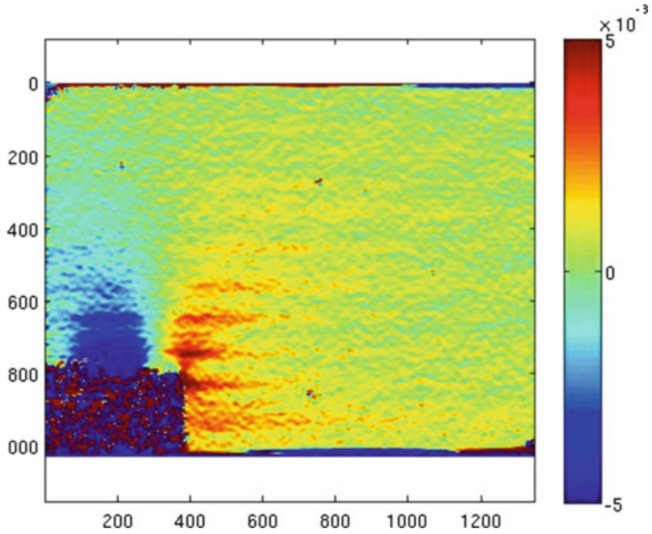

References

1. Fournely E, Moutou Pitti R, Bouchair A (2012) Behaviour of timber lattice beam with semi-rigid joints: analytical and experimental study. Pro Ligno 8:19–41
2. Fournely E, Moutou Pitti R, Bouchair H, Dubois F (2012) Experimental analysis of the semi-rigidity joint in the standardized timber beam. Springer 34:357–366. doi:10.1007/978-1-4614-4226-4_42
3. AFNOR, NF EN 408 (2004) Structures en bois, Bois de structure et bois lamellé collé, détermination de certaines propriétés physiques et mécaniques. Mars, p 32
4. Leichti RJ, Hyde RA, French ML, Camillos SG (2000) The continuum of connection rigidity in timber structures. Wood Fiber Sci 32:1–19
5. Méité M, Dubois F, Pop O, Absi J (2013) Mixed mode fracture properties characterization for wood by digital images correlation and finite element method coupling. Eng Fract Mech 105:86–100
6. Badulescu C, Grédiac M, Mathias J-D (2009) Investigation of the grid method for accurate in-plane strain measurement. Meas Sci Technol 20(9):095102. doi:10.1088/0957-0233/20/9/095102
7. Moutou Pitti R, Badulescu C, Grédiac M (2014) Characterization of a cracked specimen with full-field measurements: direct determination of the crack tip and energy release rate calculation. Int J Fract. doi:10.1007/s10704-013-9921-5
8. Lachhab A, Moutou Pitti R, Toussaint E, Grédiac M (2014) Evaluation of energy release rate in dried wood material using the grid method. In: ECWM7, seventh European conference on wood modification, Lisbone, Spain, 10–12 March 2014
9. AFNOR, Eurocode 5 (2005) Conception et calcul des structures en bois—généralités, règles communes et règles pour les bâtiments, NF EN 1995-1.1
10. Piro JL, Grédiac M (2004) Producing and transferring low-spatial-frequency grids for measuring displacement fields with moiré and grid methods. Exp Tech 28(4):23–26